Journal of Marine Systems, 1 (1990) 1–11
Elsevier Science Publishers B.V., Amsterdam – Printed in The Netherlands

Unstable and damped modes in coupled ocean mixed layer and cloud models

P.C. Chu [1], R.W. Garwood, Jr. [1] and P. Muller [2]

[1] *Department of Oceanography, Naval Postgraduate School, Monterey, CA 93943 (U.S.A.)*
[2] *Department of Oceanography, University of Hawaii, Honolulu, HI 96822 (U.S.A.)*

Received September 16, 1989; revised version accepted November 24, 1989

ABSTRACT

Chu, P.C., Garwood, R. and Muller, P., 1990. Unstable and damped modes in coupled ocean mixed layer and cloud models. J. Mar. Syst., 1: 1–11.

The ocean mixed layer and clouds are coupled by the fluxes of momentum, heat, and water mass at the interface. The importance of the fluxes of momentum and heat is well recognized by both meteorologists and oceanographers. However, the water mass flux has been given considerable attention only in atmospheric models since the latent heat release is an important source of energy for the atmospheric general circulation. The water mass flux is given less attention in ocean models although it is realized that evaporation and precipitation contribute to the surface buoyancy flux which influences the depth of mixing and the thermohaline circulation.

Clouds and the ocean mixed layer are coupled by both the heat and moisture fluxes across the air–ocean interface. Two time scales are demonstrated in this paper: a sea surface temperature (SST) evolution time scale, τ_T, that is virtually controlled by the oceanic planetary boundary layer (OPBL) and a cloud-SST coupling time scale, $\tau_{n,T}$. These two time scales depend on the stability of the marine atmospheric boundary layer (MABL). The more unstable the atmosphere, the shorter the time scales will be. For a stable atmosphere, $\tau_T \sim 1$–3 years, and $\tau_{n,T} \sim 0.3$–1 years. However for an unstable atmosphere, $\tau_T \sim 20$–30 days, and $\tau_{n,T} \sim 3$–6 days.

An air–ocean coupled model is presented in this paper for two different regimes: (1) the non-entraining ocean mixed layer case and (2) the entraining mixed layer case. The model results demonstrate that the exchanges of heat and water across the sea surface lead to both growing and decaying modes of oscillation on the two time scales due to the stability of the atmosphere. These oscillatory solutions are entirely thermodynamic and do not require wave dynamics for their existence.

Introduction

Since 1970 significant progress has been made both in our ability to carry out air–sea interaction field work and in our understanding of many of the processes found on both sides of the air–sea interface. Many studies, both observational and theoretical, have shown that the surface wind and the SST are two important elements in the air–sea coupled system (Chu, 1989).

The feedback mechanism between clouds and ocean mixed layer can be explained as follows. First, clouds reduce the incoming solar radiation at the ocean surface by scattering and absorption, which cools (relatively) the ocean surface layer by increasing mixed layer entrainment. The cooling of the ocean mixed layer lowers the evaporation rate, which will diminish the clouds. This is a negative feedback mechanism. Second, precipitation dilutes the surface salinity, stabilizing the upper ocean and reducing mixed layer deepening. The mixed layer may be caused to shallow if the downward surface buoyancy flux is sufficiently enhanced by the precipitation. The reduction in

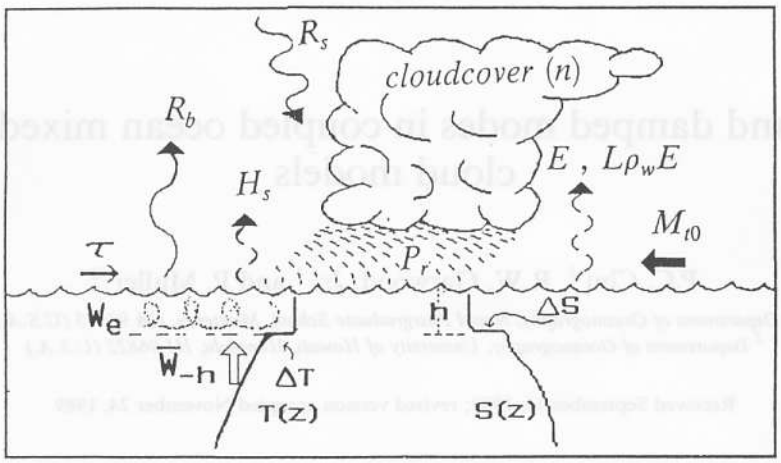

Fig. 1. Main physical processes in the two adjacent boundary layers.

mixed layer depth will increase the sea surface temperature by concentrating the net radiation plus heat fluxed downward across the sea surface into a thinner layer. The increase of SST augments the surface evaporation, which in turn produces more clouds. This is a positive feedback mechanism. Figure 1 shows the main physical processes and fluxes of heat, mass and momentum in the OPBL and the marine atmospheric boundary layer. Figure 2 illustrates the feedback pathways between the clouds and the ocean mixed layer (Chu and Garwood, 1989).

The feedback mechanism between clouds and ocean mixed layer largely depends on the dynamics of ocean mixed layer. Ocean surface buoyancy flux either generates or dampens the turbulent kinetic energy in the upper ocean depending upon the direction of the flux. Upward buoyancy flux tends to cause the water column to be statically unstable, which generates turbulence. On the otherhand, downward buoyancy flux makes the water column to be statically stable, damping the turbulence. In the case of upward buoyancy flux, or in the case when the shear production exceeds the buoyant damping, the mixed layer entrains water from below, increasing the potential energy. If there is sufficiently strong downward buoyancy flux, the shear production may be insufficient to overcome the buoyant damping and turbulence cannot reach the former mixed layer depth, causing mixed layer retreat (damping regime). It is expected that the effect of clouds on the ocean mixed layer is different for these two oceanic regimes.

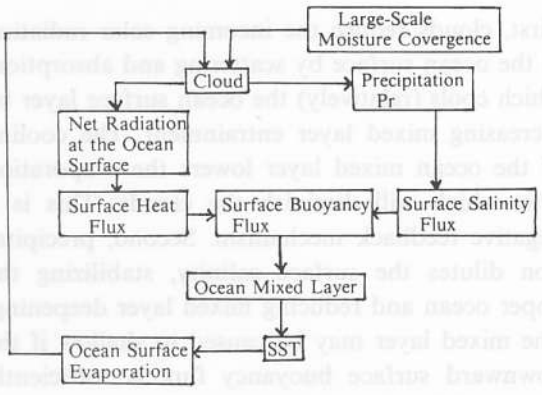

Fig. 2. Feedback paths between OPBL and clouds.

Since clouds have significant effects on the large-scale atmospheric circulation through the transfer of heat, moisture and momentum and on the ocean mixed layer through the attenuation of solar radiation at the ocean surface, and since the SST is an important factor for the development of clouds, the feedback mechanism mentioned above has a potentially significant importance for air–sea interaction, weather and ocean prediction.

Although our coupled model is one-dimensional, we are aware of the importance of horizontal advection and the limitation of one-dimensional models. However, the intent of this work is to develop a formalism to examine thermodynamic feedback between the two fluids. Because we wish to concentrate on the thermodynamic

interaction, horizontal advection is ignored initially.

Atmospheric model

Atmospheric surface layer

Using similarity theory, if a variable (wind, temperature, or moisture, etc.) is appropriately scaled, then its vertical profile follows a universal function whose form, in general, may be determined empirically. For the barotropic atmosphere the appropriate scales for wind speed and boundary layer height are

$$U = U_g,\ h_a \sim \frac{u_{a*}}{|f|} \tag{1}$$

where U_g is the geostrophic wind speed, which is assumed here to be 10 m/s, f is the Coriolis parameter and u_{a*} is the atmospheric friction velocity. Using the similarity functions $\tilde{a}$, $\tilde{b}$ and $\tilde{c}$, the geostrophic drag coefficient C_g is computed by Yamada (1976) as

$$C_g = \frac{u_{a*}}{|U_g|} = \kappa \left\{ \left[\ln\left(\frac{h_a}{z_0}\right) - \tilde{a} \right]^2 + \tilde{b}^2 \right\}^{-1/2} \tag{2}$$

where κ is the von Karman constant, 0.4. The roughness parameter, z_0, is approximately 1.5×10^{-4}m. The ratio h_a/z_0 is 0.6×10^7 for an MABL height, $h_a = 1$ km. The heat and moisture transfer coefficients are determined by

$$C_H = -\frac{\overline{w_a'\theta'}|_0}{u_{a*}[\hat{\theta} - \theta(z_0)]},\quad C_E = -\frac{\overline{w_a'q'}|_0}{u_{a*}[\hat{q} - q(z_0)]} \tag{3}$$

where w, θ, q are the vertical velocity, potential temperature and specific humidity, respectively. Here the symbol "$\hat{}$" denotes the values being taken at the top of the MABL. The heat transfer coefficient is given by

$$C_H = \frac{\kappa}{Pr_0}\left[\ln\left(\frac{h}{z_0}\right) - \tilde{c} \right]^{-1} \tag{4}$$

where Pr_0 is the turbulent Prandtl number for neutral stability, having a value of 0.74 according to Businger et al. (1971). Based on the Wangara data, the similarity functions $\tilde{a}$, $\tilde{b}$, $\tilde{c}$ are experimentally determined for the stable atmosphere (Yamada, 1976):

$$\tilde{a} = 1.855 - 0.38 h_a/L_a \quad (0 \leqslant h_a/L_a \leqslant 35),$$

$$\tilde{a} = -2.94(h_a/L_a - 19.94)^{1/2} \quad (35 < h_a/L_a);$$

$$\tilde{b} = 3.02 + 0.3 h_a/L_a \quad (0 \leqslant h_a/L_a \leqslant 35),$$

$$\tilde{b} = 2.85(h_a/L_a - 12.47)^{1/2} \quad (35 < h_a/L_a);$$

$$\tilde{c} = 3.665 - 0.829 h_a/L_a \quad (0 \leqslant h_a/L_a \leqslant 18),$$

$$\tilde{c} = -4.23(h_a/L_a - 11.21)^{1/2} \quad (18 < h_a/L_a) \tag{5a}$$

and for the unstable atmosphere ($h_a/L_a < 0$):

$$\tilde{a} = 10.0 - 8.145(1 - 0.008376 h_a/L_a)^{-1/3},$$

$$\tilde{b} = 3.02(1 - 3.29 h_a/L_a)^{-1/3},$$

$$\tilde{c} = 12.0 - 8.335(1 - 0.03106 h_a/L_a)^{-1/3} \tag{5b}$$

where L_a is the atmospheric Obukhov length scale. It is noteworthy that the formulae (5a,b) were obtained form the Wangara atmospheric boundary layer over land rather than from the MABL. There have been no comparable observations in the MABL as yet. Nevertheless, we assume that these similarity functions (5a,b) are valid for the MABL. Furthermore, since the computation method for the moisture transfer coefficient is not well established, in this paper we assume that

$$C_E = C_H \tag{6}$$

Substitution of (5a,b) into (2) and (4) leads to the apparently strong dependence of C_g, C_H, C_E on the atmospheric stability parameter h_a/L_a, as shown in Fig. 3. These parameters have much larger values for the unstable atmospheric than for the stable atmosphere, i.e.,

$$C_g \sim 0.0316,\ C_H,\ C_E \sim 0.063 \ (h_a/L_a < 0)$$

$$C_g \sim 0.003,\ C_H,\ C_E \sim 0.004 \ (h_a/L_a > 0) \tag{7}$$

Simple cloud model

The time rate of change of cloud cover is proportional to the moisture supply divided by the amount of water vapor necessary to produce the model cloud. The main processes causing the cloud dissolution are precipitation and mixing with the environmental air. The cloud evaporation due to mixing with ambient air is a complicated problem,

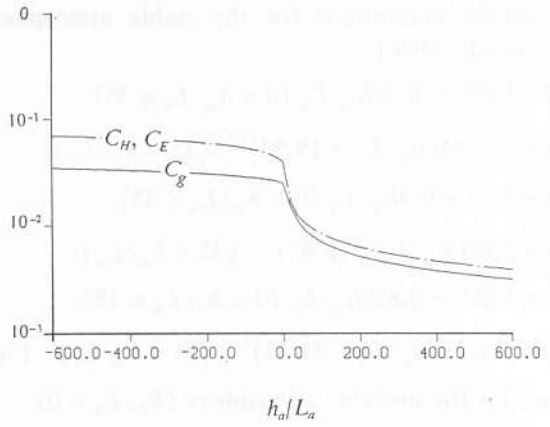

Fig. 3. Dependence of C_g, C_H, C_E on the atmospheric stability parameter (h_a/L_a).

and is neglected for the sake of simplicity here. Thus the equation for cloud cover is reduced to

$$\frac{\partial n}{\partial t} = \frac{(M_{t0} + E - P_r)}{h_c} \tag{8}$$

where h_c is the total amount of water vapor needed to create the cloud over a unit area, M_{t0} is the large-scale horizontal moisture convergence in the column of atmosphere per unit area, E is the surface evaporation rate and P is the precipitation rate. From mean distributions of temperature and mixing ratio in the environmental air outside the cloud and inside a deep cumulus cloud (Kuo, 1965), we estimate that $h_c \sim 5$ cm.

Relationship between precipitation rate and cloud cover

By linear regression of hourly rain amounts and satellite IR brightness data obtained during Phases I, II and III of GATE, Albright et al. (1985) suggested a linear relationship between average precipitation rate P_r in boxes on a side and cloud cover n of the boxes by clouds with tops colder than $-36\,^\circ$C:

$$P_r(\mathrm{ms}^{-1}) = (0.472 + 8.333n) \times 10^{-7} \tag{9}$$

This result verified Arkin's (1979) earlier analysis for the GATE B-scale array.

Cloud effects on the net radiation at the ocean surface

Clouds reduce the solar radiation incident at the ocean surface by scattering and absorption. These effects are included in Budyko's (1978) formula

$$R_s = [1 - \alpha_{sn}n - \alpha_{s0}(1 - n)]\, R_{s0} \tag{10}$$

Here R_{s0} (340 W m^{-2}) is the solar radiation absorbed by the ocean surface layer under a clear sky. The parameters α_{sn} and α_{s0} represent albedos of the earth–atmosphere system with complete cloud cover and a cloudless sky, respectively, and have the following values:

$$\alpha_{sn} = 0.46,\ \alpha_{s0} = 0.2$$

The ocean surface emits longwave radiation to the atmosphere and to space. However, clouds, as well as dry air, partially absorb the radiation and re-emit longwave radiation back to the ocean surface. Thus the net upward energy loss by longwave radiation at the ocean surface, R_b, is corrected for the downward radiation by the clouds and the air. From longwave radiation data, Budyko (1978) derived a semi-emprical formula:

$$R_b = a + bT - (a_1 + b_1)n \tag{11}$$

The dimensional coefficients a, b, a_1 and b_1 are

$$a = -377.6\ \mathrm{Wm}^{-2},\ b = 2.2\ \mathrm{Wm}^{-2}\mathrm{K}^{-1},$$
$$a_1 = -389.8\ \mathrm{Wm}^{-2},\ b_1 = 1.6\ \mathrm{Wm}^{-2}\mathrm{K}^{-1}$$

The effects of clouds on buoyancy flux at ocean surface

For the case of an ocean surface without ice (low and middle latitudes) the surface buoyancy flux, B, has two components:

$$B = -\frac{\alpha g F}{\rho_w c_{pw}} - \beta g(E - P_r)S \tag{12}$$

Here α is the sea water thermal expansion coefficient, β is the salinity contraction coefficient, ρ_w is the water density and c_{pw} is the sea water specific heat under constant pressure. The surface heat flux, F (upward positive), is computed by

$$F = R_b - R_s + L\rho_w E + H_s \tag{13}$$

where L is the latent heat of vaporization and H_s is the sensible heat flux to the air. The variables T_{-h} and S_{-h} are the temperature and salinity of the water immediately below the mixed layer that may be entrained into the mixed layer. Standard

bulk formulae are used to calculate the surface evaporation:

$$E = \rho_a C_D U_g C_E \left[q_s(T_w) - \hat{q} \right] / \rho_w \tag{14}$$

and the sensible heat flux from the ocean surface:

$$H_s = \rho_a c_{pa} C_D U_g C_H \left(T_w - \hat{\theta} \right) \tag{15}$$

where $q_s(T)$ is the saturated mixing ratio, c_{pa} is specific heat of the atmosphere, and $\hat{\theta}$ and $\hat{q}$ are the air temperature and mixing ratio at the top of the MABL.

The effect of clouds on the buoyancy flux at the ocean surface is two-fold: (1) decreasing B through the increase in the net heat loss at the ocean surface, F, by reducing the incoming solar radiation and (2) increasing B due to precipitation.

Ocean mixed layer model

Most models which include thermodynamic effects regard the upper layer as a well-mixed turbulent boundary layer which exchanges heat and moisture with the atmosphere and entrains water from below. The heat and salinity equations take the forms

$$h_w \frac{\partial T_w}{\partial t} = -w_e (T_w - T_{-h}) - \frac{F}{\rho_w c_p^{(w)}} + A_T \tag{16}$$

$$h_w \frac{\partial S}{\partial t} = -w_e (S - S_{-h}) + (E - P_r) S + A_S \tag{17}$$

where h_w is the mixed layer depth and A_T and A_s are the horizontal advection for temperature and salinity, respectively. The entrainment velocity is w_e and is parameterized as (Chu and Garwood, 1988):

$$w_e = \Lambda \frac{\left(C_1 u_{w*}^3 - C_2 Bh \right)}{gh \left[\alpha (T_w - T_{-h}) - \beta (S - S_{-h}) \right]} \tag{18}$$

where C_1 and C_2 are tuning coefficients and u_{w*} is the water surface friction velocity, which is computed by

$$u_{w*} = \left(\frac{\rho_a}{\rho_w} \right)^{1/2} u_{a*} \tag{19}$$

for an atmospheric friction velocity of 30 cm/s, $u_{w*} \sim 1.1$ cm/s. The symbol Λ is a Heaviside function of $(C_1 u_{w*}^3 - C_2 Bh)$. When $(C_1 u_{w*}^3 - C_2 Bh) > 0$ there is sufficient turbulent kinetic energy to entrain and mix water from below and

$$\Lambda = 1$$

which represents the entrainment regime. The entrainment rate is determined by (18) and substituted into the following equation to prognosticate the mixed layer depth h.

$$\frac{\partial h}{\partial t} = w_e - w_{-h} \tag{20a}$$

Here w_{-h} is the vertical velocity at the mixed layer base.

When $(C_1 u_*^3 - C_2 Bh) < 0$ there is not enough turbulent kinetic energy to entrain water from below, w_e is set to be zero, i.e.,

$$\Lambda = 0$$

which is called the surface damping regime. The mixed layer depth is calculated diagnostically from a balance of the remaining terms in (18) and it equals the oceanic Obukhov length scale, L_w:

$$h_w = L_w = \frac{C_1 u_{w*}^3}{C_2 B} \tag{20b}$$

One example for the surface damping regime is the western Pacific warm pool region where the excess precipitation effect prevails over the buoyancy loss effect of heat loss at the ocean surface, causing the net buoyant flux to be downward.

The temperature and salinity equations (16) and (17) describe the balance of storage, entrainment and heating/water mass flux.

Basic equations for perturbations

The mean state of the coupled cloud-OPBL system ($\overline{T}_w$, $\overline{S}$, $\overline{h}$, $\overline{E}$, $\overline{P}_r$, $\overline{w}_e$) is evaluated from the steady-state solutions for the prognostic equations (8), (16), (17) and (20a).

When the coupled system is perturbed from its equilibrium state, the thermodynamic feedback mechanism between the cumulus clouds and the oceanic mixed layer causes the perturbation to either grow (positive feedback) or dampen (negative feedback). The principal purpose here is to study possible one-dimensional thermodynamic feedback mechanisms between clouds and the oceanic mixed layer, within the limitations of the

simplifying assumptions. Hence the energy exchange at the air–ocean interface is a primary focal point. Therefore, we shall neglect initially the perturbations of those variables which are not directly related to the exchange at the air–ocean interface, such as the perturbations of the horizontal advection A'_T and A'_s, the perturbations of the atmospheric variables at the top of the MABL, $\hat{q}'$ and $\hat{\theta}'$ and the perturbations of the oceanic variables at the base of the OPBL, w'_{-h}, T'_{-h} and S'_{-h}. From the basic equations of the coupled system (8), (16), (17) and (20a or b), the perturbation of cloud cover, n', is given by

$$\frac{\partial n'}{\partial t} = \frac{1}{\bar{h}_c}\left(\frac{\partial \bar{E}}{\partial T_w} T'_w - \frac{\partial \bar{P}_r}{\partial n} n'\right) \tag{21}$$

The equations for T'_w, S', are

$$\frac{\partial T'_w}{\partial t} = -\frac{1}{\rho_w c_{pw} \bar{h}_w}\left(\frac{\partial \bar{F}}{\partial n} n' + \frac{\partial \bar{F}}{\partial T_w} T'_w - \frac{\bar{F}}{\bar{h}_w} h'_w\right) - \Lambda\left(\frac{\bar{w}_e}{\bar{h}} T'_w + \frac{\Delta T}{\bar{h}} w'_e\right) \tag{22}$$

$$\frac{\partial S'}{\partial t} = \frac{(\bar{E} - \bar{P}_r)}{\bar{h}_w} S' + \frac{\bar{S}}{\bar{h}_w}(E' - P'_r) + \frac{(\bar{P}_r - \bar{E})\bar{S}}{\bar{h}_w^2} h'_w - \Lambda\left(\frac{\bar{w}_e}{\bar{h}} S' + \frac{\Delta S}{\bar{h}} w'_e\right) \tag{23}$$

The equation for h'_w has different forms for the two regimes. For the entrainment regime it has the prognostic form

$$\frac{\partial h'}{\partial t} = w'_e \tag{24a}$$

where

$$w'_e \, \Delta b = -g\bar{w}_{-h}(\alpha T'_s - \beta S'_s) - C_1 \frac{\bar{u}^3_*}{\bar{h}^2} h' + C_2 B' \tag{25}$$

For the surface damping regime, it has the diagnostic form

$$h'_w = -\frac{\bar{h}_w}{\bar{B}} B' = \frac{\bar{h}_w}{\bar{B}}\left[\left(\frac{\alpha g}{\rho_w c_{pw}} \frac{\partial \bar{F}}{\partial T_w} + \beta g \bar{S} \frac{\partial \bar{E}}{\partial T_w}\right) T'_w - \beta g \bar{S}(\bar{P}_r - \bar{E}) S' + \left(\frac{\alpha g}{\rho_w c_{pw}} \frac{\partial \bar{F}}{\partial n} - \beta g \bar{S} \frac{\partial \bar{P}_r}{\partial n}\right) n'\right] \tag{24b}$$

From (9) and (14) E' and P'_r are computed by

$$E' = \frac{d\bar{E}}{dT_w} T'_w, \quad P'_r = \frac{\partial \bar{P}_r}{\partial n} n' \tag{26}$$

Three basic time scales

Three time scales are found from (21)–(24):

(a) Cloud time scale

$$\tau_n^{-1} = \frac{1}{h_c} \frac{\partial \bar{P}_r}{\partial n} \tag{27}$$

Using (9) and taking $h_c = 5$ cm, we have

$\tau_n \sim 0.6$ day

(b) SST variation time scale

$$\tau_T^{-1} \equiv \frac{1}{\rho_w c_{pw} \bar{h}_w} \frac{\partial \bar{F}}{\partial T_w} \tag{28}$$

Based on the assumption that $\hat{\theta}$ and $\hat{q}$ are determined by the large-scale atmospheric motion only, from the heat balance (13) we have

$$\frac{\partial \bar{F}}{\partial T_w} = \rho_a c_{pa} U_g \left(1 + \frac{L^2 q_s}{c_{pa} R_v T_w^2} \frac{C_E}{C_H}\right) C_g C_H$$

Therefore

$$\tau_T^{-1} = \frac{\rho_a c_{pa} U_g}{\rho_w c_{pw} \bar{h}_w}\left(1 + \frac{L^2 q_s}{c_{pa} R_v T_w^2} \frac{C_E}{C_H}\right) C_g C_H \tag{29}$$

Cloud and SST coupling time scale

$$\tau_{n,T}^{-1} \equiv \frac{1}{\rho_w c_{pw} \bar{h}_w} \frac{\partial \bar{F}}{\partial n} \frac{\partial \bar{E}}{\partial T_w} \Big/ \frac{\partial \bar{P}_r}{\partial n}$$

Utilization of (27) leads to

$$\tau_{n,T}^{-1} = \left[\frac{\tau_n U_G L q_s \dfrac{\partial F}{\partial n}}{\rho_w c_{pw} h_w h_c R_v T_w^2}\right] C_g C_E \tag{30}$$

Using (10), (11) and (13) we have

$$\frac{\partial F}{\partial n} = \frac{\partial (R_b - R_s)}{\partial n} \sim 15 \mathrm{Wm}^{-2}$$

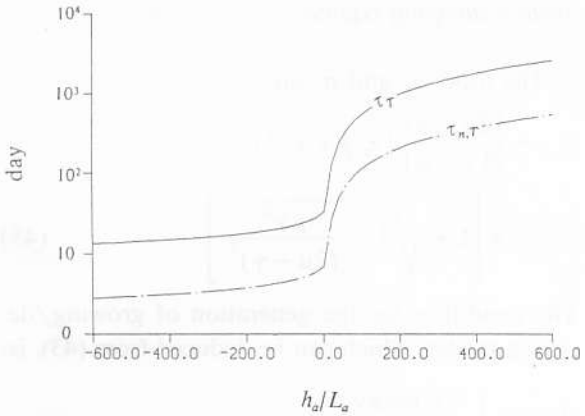

Fig. 4. Dependence of τ_T and $\tau_{n,T}$ on the atmospheric stability parameter (h_a/L_a).

Among these three times scales, τ_n is the shortest. The other two, τ_T and $\tau_{n,T}$, largely depend on the parameters C_g, C_H and C_E, which are functions of the atmospheric stability. Figure 4 shows the dependence of τ_T and $\tau_{n,T}$ on the atmospheric stability. For the unstable atmosphere $(h_a/L_a < 0)$, $\tau_{n,T} \sim$ 3–6 days and $\tau_T \sim$ 20–30 days. For the stable atmosphere $(h_a/L_a > 0)$, $\tau_{n,T} \sim$ 0.3–1 years and $\tau_T \sim$ 1–3 years.

Since the time scale for cloud feedback is so much shorter than that for SST feedback, i.e., $\tau_n \ll \tau_T$, the cloud cover perturbation, n', almost instantaneously follows the SST for the temperature feedback:

$$n' = \frac{\partial \bar{E}/\partial T_w}{\partial \bar{P}_r/\partial n} T_w' \tag{31}$$

Equation (9) shows that

$$\frac{\partial \bar{P}_r}{\partial n} \sim 8.33 \times 10^{-7} \mathrm{ms}^{-1}, \tag{32}$$

and for $\bar{T}_w = 25\,^\circ\mathrm{C}$, $u_{a*} = 0.1$ m/s,

$$\frac{\partial \bar{E}}{\partial T_w} = C_E u_{a*} \frac{\mathrm{d}q_s(\bar{T}_w)}{\mathrm{d}T_w} \sim 4.63 \times 10^{-7} \mathrm{ms}^{-1}\mathrm{K}^{-1}.$$

$$\frac{\partial \bar{E}/\partial T_w}{\partial \bar{P}_r/\partial n} \sim 0.56 \mathrm{K}^{-1} \tag{33}$$

Therefore, a 1°C change in SST implies a 0.56 change in cloud cover.

Surface damping regime

Neglecting the small terms in the prognostic equation for T_w' and S' and eliminating three among the four variables n', T_w', S' and h_w' from (22), (23), (24b), (31), we obtain the second order differential equation,

$$\frac{\partial^2 \psi}{\partial t^2} - \frac{2\mu - \gamma}{\gamma - \mu}\left(\tau_{n,T}^{-1} + \tau_T^{-1}\right)\frac{\partial \psi}{\partial t} + \frac{\mu\gamma^2}{(\gamma - \mu)^2}\left(\tau_{n,T}^{-1} + \tau_T^{-1}\right)^2 \psi = 0 \tag{34}$$

where ψ represents n', T_w', S' and h_w'. There are two nondimensional parameters,

$$\mu = \frac{4\alpha g \bar{F}/\rho_w c_{pw}}{\beta g \bar{h}_w \bar{S}\left(\tau_{n,T}^{-1} + \tau_T^{-1}\right)},$$

$$\gamma = \frac{4\beta g\left(\bar{P}_r - \bar{E}\right)\bar{S}}{\beta g \bar{h}_w \bar{S}\left(\tau_{n,T}^{-1} + \tau_T^{-1}\right)} \tag{35}$$

that indicate the relative importance of mean heat and mean salinity fluxes in the mean surface buoyancy flux B.

Entrainment regime

In the entrainment regime, the four variables n', T_w', S', w_e' and h_w' are obtained from three prognostic equations (22), (23) and (24a), and two diagnostic equations (31) and (25). Eliminating four variables from these five equations we obtain third-order differential equation:

$$\left(\frac{\partial^3}{\partial t^3} + a_1 \frac{\partial^2}{\partial t^2} + a_2 \frac{\partial}{\partial t} + a_3\right)\psi = 0 \tag{36}$$

where a_1, a_2, a_3 are functions of the following two parameters (Chu and Garwood, 1989):

$$\lambda \equiv \frac{1}{g h_c} \frac{\partial B}{\partial n} \tag{37a}$$

which is the dependence of the surface buoyancy flux change on cloud cover and

$$\kappa \equiv \frac{\alpha g\, \Delta T}{\Delta b} \tag{37b}$$

which is the fraction of the mixed layer base density jump induced by temperature to the total density jump. Here

$$\Delta b = g(\alpha\, \Delta T - \beta\, \Delta S) \tag{38}$$

is the reduced gravity, and ΔT and ΔS are the mean temperature and salinity jumps at the base of the ocean mixed layer:

$$\Delta T \equiv \overline{T}_w - T_{-h},\ \Delta S \equiv \overline{S} - S_{-h} \tag{39}$$

Solutions

It is noteworthy that the entrainment regime (36) is of the third order, whereas the damping regime (34) is of the second order because of the change between prognostic and diagnostic form for the respect of mixed layer depth equations (24a,b). The general solutions of the two regimes have the form:

$$\psi = \sum d_j \exp(\sigma_j t) \tag{40}$$

where d_j ($j = 1, 2, \ldots$) are the integral constants and σ_j (j = 1, 2, ...) are eigenvalues. In the solution (40), there are two terms for the surface damping regime and three terms for the entrainment regime. For the surface damping regime, the eigenvalues are the roots of the second-order algebraic equation

$$\sigma^2 - \frac{2\mu - \gamma}{\gamma - \mu}\left(\tau_{n,T}^{-1} + \tau_T^{-1}\right)\sigma + \frac{\mu\gamma^2}{(\gamma - \mu)^2}\left(\tau_{n,T}^{-1} + \tau_T^{-1}\right)^2 = 0 \tag{41}$$

For the entrainment regime, the eigenvalues are the roots of the following third-order algebraic equation:

$$\sigma^3 + a_1\sigma^2 + a_2\sigma + a_3 = 0 \tag{42}$$

Instability and oscillation criteria

The instability criteria for the thermodynamically coupled air-ocean system are

$$\mathrm{Re}(\bar{\sigma}) \begin{cases} < 0 \text{ decaying} \\ = 0 \text{ neutral,} \\ > 0 \text{ growing} \end{cases} \tag{43}$$

where $\bar{\sigma}$ is σ_1, σ_2, or σ_3, the roots of the algebraic equations (41) or (42). The oscillation criteria for the coupled system are

$$\mathrm{Im}(\bar{\sigma}) \begin{cases} = 0 \text{ nonoscillatory} \\ \neq 0 \text{ oscillatory} \end{cases} \tag{44}$$

Surface damping regime

The roots σ_1 and σ_2 are

$$\sigma_{1,2} = \frac{(2\mu - \gamma)}{2(\overline{\gamma} - \mu)}\left(\tau_{n,T}^{-1} + \tau_T^{-1}\right) \times \left[1 \pm \sqrt{1 - \frac{\mu\gamma^2}{(2\mu - \gamma)^2}}\right] \tag{45}$$

The condition for the generation of growing/decaying modes, which can be deduced from (43), is:

$$\frac{2\mu - \gamma}{\gamma - \mu} \begin{cases} < 0 \text{ decaying} \\ = 0 \text{ neutral,} \\ > 0 \text{ growing} \end{cases} \tag{46}$$

and the condition for oscillatory/nonoscillatory modes is:

$$\left(1 - \frac{2\mu}{\gamma}\right)^2 \begin{cases} > \mu \text{ nonoscillatory} \\ < \mu \text{ oscillatory} \end{cases} \tag{47}$$

Separation of different modes in the $\gamma - \mu$ plane is shown in Fig. 5. For the buoyant damping regime ($\overline{B} > 0$, i.e., $\gamma > \mu > 0$) which corresponds to the western Pacific warm pool regime with strong precipitation, the relative importance of the mean surface heat and salinity fluxes in the mean buoyancy flux $\overline{B}$ is a key factor controlling the

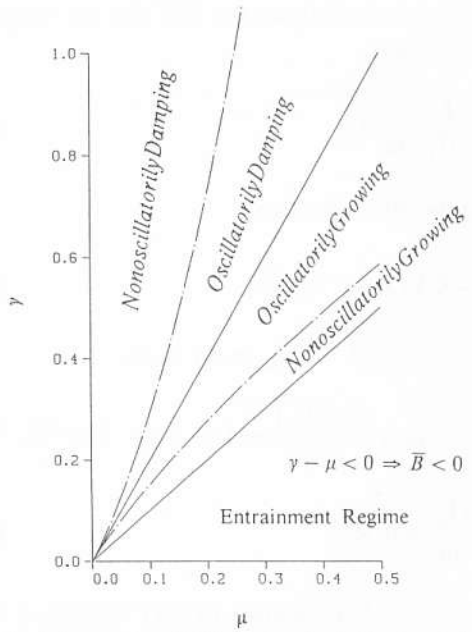

Fig. 5. Separation of different modes in the (γ,μ) plane.

modes of the coupled air-ocean system. The mean surface salinity flux, measured by γ, makes the upper ocean more buoyant and stable. However, the mean upward heat flux, measured by μ, makes the upper ocean less stable. The larger the parameter γ (μ), the stronger the negative (positive) feedback mechanism. Combining (46) and (47) leads to the results:

$$\gamma > \frac{2\mu}{1-\sqrt{\mu}} \Rightarrow \text{Nonoscillatory Damping}$$

$$\frac{2\mu}{1-\sqrt{\mu}} > \gamma > 2\mu \Rightarrow \text{Oscillatory Damping}$$

$$2\mu > \gamma > \frac{2\mu}{1+\sqrt{\mu}} \Rightarrow \text{Oscillatory Growing}$$

$$\frac{2\mu}{1+\sqrt{\mu}} > \gamma > \mu \Rightarrow \text{Nonoscillatory Growing} \quad (48)$$

Entrainment regime

For the purpose of a preliminary sensitivity analysis only κ and λ are allowed to vary, depending on observations. Other parameters are held constant as listed in Table 1. By the definition of λ (37a) and the estimates for $\partial P_r/\partial n$ (9) and Budyko's formula (10), we can estimate the value of λ as

$$\lambda \sim 0.45 \times 10^{-6}\ s^{-1}$$

which indicates that λ has an order of 10^{-6} s^{-1}. Therefore in this paper, λ varies from -10^{-6} s^{-1} to 10^{-6} s^{-1}. It is reasonable to let κ vary between -10 to 10. The case of $\kappa = 1$ means that salinity is homogeneous across the mixed layer base.

We compute all roots of (42) for different values of the parameters κ and λ, and obtain three roots at each points of the parameter space (κ, λ).

TABLE 1

Standard values for model parameters.

ρ	1.29kg/m^3	$\bar{S}$	35g/kg
C_D	10^{-3}	$\bar{h}_w$	50m
h_c	5cm	α	0.2×10^{-3} K^{-1}
$\bar{n}$	0.5	β	0.8×10^{-3}
U_g	10m/s	C_1	1.0
ρ_w	1035kg/m^3	C_2	0.2
$\bar{T}_w$	20°C	$\bar{w}_{-h}$	1 m/day

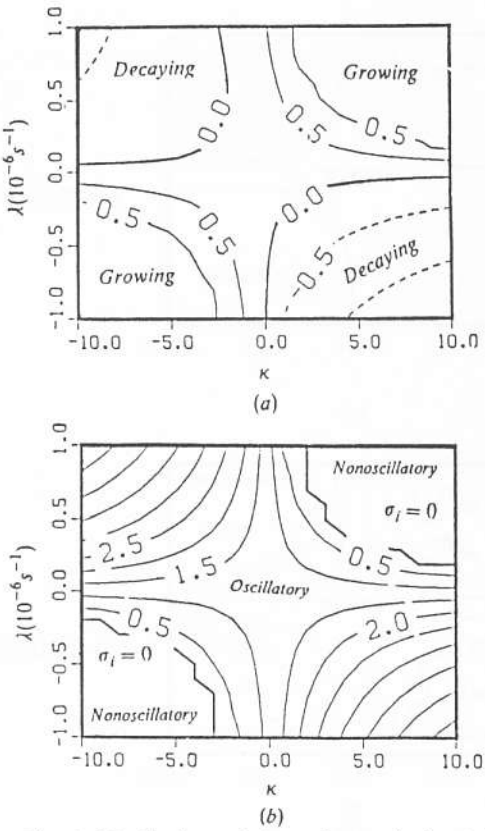

(a) Re(σ_1)

(b) |Im(σ_1)|

Fig. 6. Distributions of eigenvalue σ_1 in the (κ,λ) plane for standard case (unit in $2\pi/\tau_T$): (a) Re(σ_1), (b) |Im(σ_1)|.

One root among the three has negative real parts throughout the whole parameter space, representing the damping modes, in which we are not interested here. The other two roots, σ_1 and σ_2, have positive real parts somewhere in the parameter space, representing the existence of growing modes in certain parameter ranges. Figure 6 shows the isolines of (a) Re(σ_1) and (b) |Im(σ_1)| in the (κ,λ) plane. Figure 7 indicates the isolines of (a) Re(σ_2) and (b) |Im(σ_2)| in the (κ, λ) plane. In these figures the real and imaginary parts of the eigenvalues σ_{1r}, σ_{1i}, σ_{2r} and σ_{2i} are scaled as $2\pi/\tau_T$. Both the real part (growth rate) and the absolute value of the imaginary part (periodicity) of the roots σ_1, σ_2 show saddle-type distributions.

Several interesting results from Figs. 6 and 7 are summarized as follows:

(i) A necessary condition for the generation of growing modes, which can be seen from these figures, is:

$$\kappa\lambda > 0 \quad (49)$$

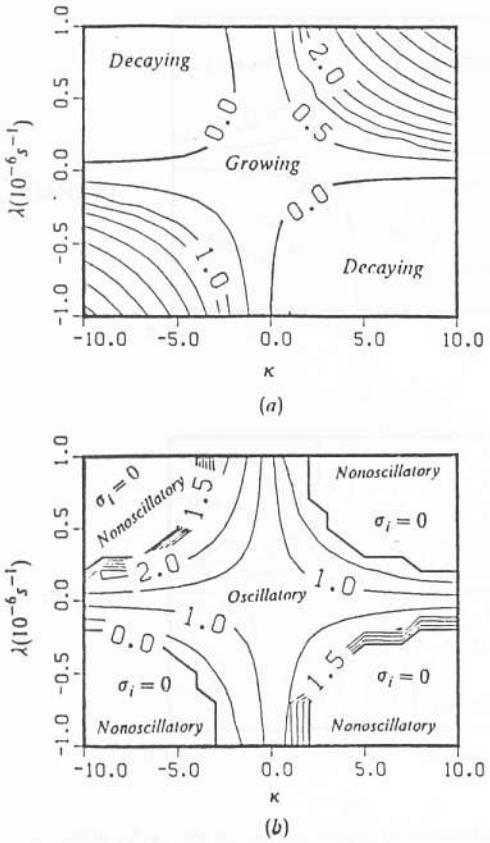

(a) $\mathrm{Re}(\sigma_2)$

(b) $|\mathrm{Im}(\sigma_2)|$

Fig. 7. Distributions of eigenvalue σ_2 in the (κ,λ) plane for standard case (unit in $2\pi/\tau_T$): (a) $\mathrm{Re}(\sigma_2)$, (b) $|\mathrm{Im}(\sigma_2)|$.

This implies that if the surface water is warmer (cooler) than the deep water, i.e., $\kappa > 0 (\kappa < 0)$, the growing modes are excited. In this case the surface buoyancy flux increases with increasing (decreasing) cloud cover.

(ii) If the damping modes are ignored, the two eigenvalues σ_1 and σ_2 exhibit the similar properties. The growing modes, σ_1 and σ_2, are further separated into oscillatory and nonoscillatory modes. The condition for this separation is given approximately by

$$\kappa\lambda \begin{cases} < A \text{ Oscillatory} \\ > A \text{ Nonoscillatory} \end{cases} \tag{50}$$

where A is a positive number of about 2×10^{-6} s^{-1}. Combining (49) with (50) and using (37a), the necessary condition for oscillatorily growing modes is

$$A > \frac{\kappa}{h_c}\frac{\partial}{\partial n}\left[\beta\bar{S}_s P_r - \frac{\alpha(R_b - R_s)}{\rho_w c_{pw}}\right]_{\bar{T}_w,\,\bar{n}} > 0 \tag{51}$$

and the condition for the nonoscillatorily growing modes is

$$\frac{\kappa}{h_c}\frac{\partial}{\partial n}\left[\beta\bar{S}_s P_r - \frac{\alpha(R_b - R_s)}{\rho_w c_{pw}}\right]_{\bar{T}_w,\,\bar{n}} > A \tag{52}$$

The properties of thermodynamic instability of the coupled system depend largely on the relationship between precipitation P_r and the cloud cover and on the relationship between net radiation at the ocean surface and the cloud cover.

(iii) The product of the two parameters κ and λ represents the relative strength of positive to negative feedback. When $\kappa\lambda$ is larger than the critical value A, the positive feedback greatly exceeds the negative feedback. The coupling system becomes nonoscillatory and growing. When $\kappa\lambda$ is positive and smaller than the critical value A, the positive feedback slightly exceeds the negative feedback. The coupled system is oscillatory and growing. When $\kappa\lambda$ is negative, the negative feedback exceeds the positive feedback. The coupled system becomes damped. Comparing Fig. 7 with Fig. 6, we find that for the oscillatory growing modes the two roots have the same growth rate and frequency. However, for the nonoscillatorily growing modes the growth rate relating to the eigenvalue σ_2 is much larger than that relating to σ_1.

(iv) For the oscillatory growing modes, the growth rate σ_r has the order of $0.5\times 2\pi/\tau_T$ and $|\sigma_i|$ has the order of $2\pi/\tau_T$. The corresponding period for the oscillation is

$$T = \frac{2\pi}{|\sigma_i|} \sim \tau_T \tag{53}$$

which means that the period of the unstable oscillation has the same order of magnitude as the SST evoluation time scale, τ_T, which is 20–30 days for the unstable atmosphere and 1–3 years for the stable atmosphere.

Conclusion

The feedback between the cloud and OPBL in the coupled MABL and stable OPBL system is investigated by a simple one-dimensional coupled model. The time scales largely depend on the stability of the MABL. For the stable atmosphere, the two time scales are quite long: $\tau_{n,T} \sim$ 100–300

days and $\tau_T \sim 1-3$ yr. For the unstable atmosphere, however, the two time scales are much shorter: $\tau_{n,T} \sim 3-6$ days and $\tau_T \sim 20-30$ days. In the western Pacific warm pool regions, the MABL is usually unstable. Therefore, this theory may provide some explanation of the two time scales (3–6 and 20–30 days) of intense convection in the western Pacific.

In the coupled system, the fresh water influx at the ocean surface due to the excess precipitation over evaporation is a damping factor (negative feedback). However, the surface cooling is a forcing factor (positive feedback). The relative strength of these two surface fluxes determine the mode type: decaying or growing, oscillatory or nonoscillatory.

Acknowledgements.

This research was supported by the National Science Foundation, the Office of Naval Research and the U.S. Naval Postgraduate School.

References

Albright, M.D., E.E. Recker, R.J. Reed and R.Q. Dang, 1985. The diurnal variation of deep convection and inferred precipitation in the central tropical Pacific during January–February 1979. Mon. Weather Rev., 113: 1663–1680.

Arkin, P.A., 1979. The relationship between fractional coverage of high cloud and rainfall accumulations during GATE over the B-scale array. Mon. Weather Rev., 107: 1382–1387.

Budyko, M.I., 1978. The heat balance of the earth. In: J. Gribbin (Editor) Climatic Change, Cambridge Univ. Press. pp. 85–113.

Businger, J.A., Wyngaard, J.C., Izumi, Y. and Bradley, E.F., 1971. Flux profile relationships in the atmospheric surface layer. *J. Atmos. Sci.*, **28**: 181–189.

Chu, P.C., 1989. Relationship between thermally forced surface wind and sea surface temperature gradient. Pure Appl. Geophys., 130: 31–45.

Chu, P.C. and R.W. Garwood, Jr., 1988. Comment on "A coupled dynamicthermodynamic model of an ice-ocean in the marginal ice zone" by Sirpa Hakkinen, J. Geophys. Res., 93: 5155–5156.

Chu, P.C. and R.W. Garwood, Jr., 1989. Cloud – ocean mixed layer feedback. AMS Symposium on the Role of Clouds in Atmospheric Chemistry and Global Climate, pp. 39–44.

Garwood, R.W. Jr., 1977. An oceanic mixed layer capable of simulating cyclic states. J. Phys. Oceanogr., 7: 455–468.

Garwood, R.W. Jr., 1979. Air–sea interaction and dynamics of the surface mixed layer. Rev. Geophys. Space Phys., 17: 1507–1524.

Kuo, H.L., 1965. On formation and intensification of tropical cyclones through latent heat release by cumulus convection. J. Atmos. Sci., 22: 40–63.

Yamada, T., 1976. On the similarity functions A, B, and C of the planetary boundary layer. J. Atmos. Sci., 33: 781–793.